COMPDYN 2015
5th ECCOMAS Thematic Conference on
Computational Methods in Structural Dynamics and Earthquake Engineering
M. Papadrakakis, V. Papadopoulos, V. Plevris (eds.)
Crete Island, Greece, 25–27 May 2015

SHEAR STRENGHT AND DEFORMATION MECHANISMS OF COMBINED AND CONFINED MASONRY WALLS SUBJECTED TO CYCLIC LOADING

Arturo Tena-Colunga[1], Artemio Juárez-Ángeles[2], and Víctor Hugo Salinas-Vallejo[3]
[1] Universidad Autónoma Metropolitana
Departamento de Materiales
Av. San Pablo 180, 02200 México, DF, MEXICO
e-mail: atc@correo.azc.uam.mx

[2] ICA Ingeniería
México, DF, MEXICO
e-mail: arjuan_uam@hotmail.com

[3] EuroEstudios
México, DF, México
e-mail: vicusalva@hotmail.com

Keywords: Confined Masonry, Combined Masonry, Shear Strength, Deformation Capacity, Cyclic Testing.

Abstract. *The experimental masonry research in Mexico has concentrated in confined masonry walls, primarily those made with brick, However, a modality named as "combined and confined masonry", where courses of lightweight concrete blocks (cheap in Mexico), are alternated with courses of bricks (more expensive) is being widely used in seismic zones of Mexico. Since there were no tests available for the described combined and confined masonry walls, Mexicans have no information about the performance of such walls under alternated earthquake loading. Therefore, an experimental program was needed in order to evaluate the strength and deformation mechanisms of such walls subjected to cyclic loading. The results of the first cycling testing conducted for combined and confined masonry walls are reported in this paper. The cyclic testing followed the protocol established by Mexican guidelines, which is similar to that used worldwide for the cyclic testing of wall structures. The research not only evaluates resisting mechanisms and deformation characteristics of such walls, but also defines values of useful parameters for analysis and design.*

1 INTRODUCTION

The great demand of housing in Mexico for low income people living in small cities, towns and suburbs, has forced these people to look for alternative constructive systems that would allow them to build their homes with a reduced budget, using then some of the cheapest materials available. One of the new systems used for this purpose is what we call here "combined and confined masonry", where courses of lightweight concrete blocks (cheap in Mexico), are alternated with courses of bricks (more expensive), as depicted in Figure 1. This type of masonry construction allows important saving in costs and execution time, besides having an aesthetic appearance.

a) 3 bricks courses by 1 block course

b) 2 brick courses by 1 block courses

c) 3 brick courses by 3 block courses

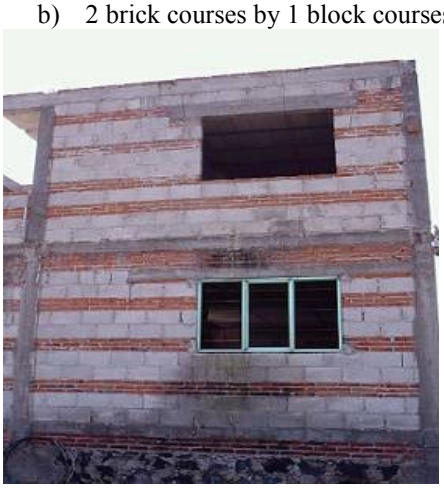

d) 3 brick courses by 2 block courses

Figure 1. Combined and confined masonry construction

This modality of construction has historical background in old construction in Europe in places like Istanbul, Turkey or Athens, Greece (Figure 2) and in few buildings of the XVII or XVIII century in Mexico (Figure 3), where natural stones were alternated with fired bricks. However, this newer version became popular in recent times by the initiative of the inhabitants of the Mexican states of Puebla, Tlaxcala and Oaxaca. They tried to solve with this modality the cracking problem observed in walls made with concrete blocks due to differential settlements. As a matter of fact, their idea of alternating courses of bricks with concrete blocks was successful to solve that problem.

a) Acropolis Archeological site area b) Acropolis Museum area

Figure 2. Existing old combined masonry buildings in Athens, Greece

a) Downtown Mexico City b) Downtown Mérida

Figure 3. Existing old combined masonry buildings in México

This modern version of combined and confined masonry has been being used since early 1990s. Different arrangements to combine and alternate brick courses with block courses have been used [1-4, Figure 1], but the one that it is more commonly used is the one depicted in Figure 1a, where three courses of clay bricks alternate with a course of concrete blocks.

Previous experimental masonry research in Mexico that started in the late 1960s has concentrated in confined masonry walls, primarily those made with brick [for example, 5-10], although there are also some testing with confined walls made with concrete blocks [for example, 11]. Since there were no tests available for the described combined and confined masonry walls, Mexicans have no information about the performance of such walls under alternated earthquake loading, other than the satisfactory performances observed for one and two stories houses at small towns in Puebla and Tlaxcala states during the moderate June 15, 1999 Tehuacán earthquake (M=6.5). The described system is being used in seismic regions of Mexico where the earthquake hazard is high, and the number of applications is growing very fast. In fact, this system is starting to be used in Mexico City as well. Therefore, an experimental program was needed in order to evaluate the strength and deformation mechanisms of such walls when subjected to strong lateral cyclic loading.

The results of the first cycling testing conducted for combined and confined masonry walls are reported in this paper. The cyclic testing followed the protocol established by Mexican guidelines, which is similar to that used worldwide for the cyclic testing of wall structures.

The research not only evaluates resisting mechanisms and deformation characteristics of such walls, but also defines values of useful parameters for analysis and design.

2 MATERIAL PROPERTIES

The combined and confined masonry construction currently used in Mexico for non-engineered construction is composed of non-industrial fired clay bricks and lightweight concrete blocks with no quality control, which dimensions are depicted in Figure 4.

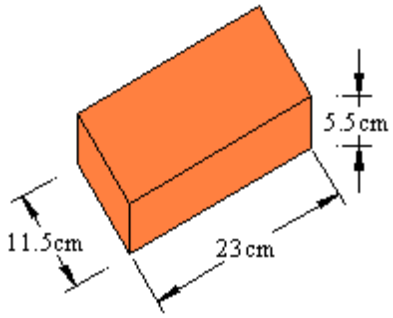

a) Typical clay brick used

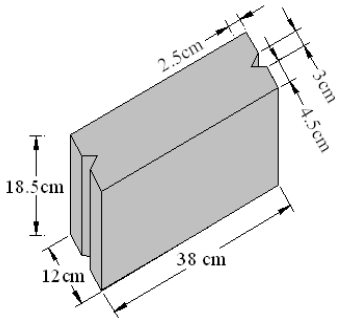

b) Typical concrete block used

Figure 4. Pieces commonly used in recent combined and confined masonry construction

The mortar bed joint ranges from 1 cm (3/8") to 1.5 cm (5/8") in thickness. Head joints are filled with mortar and they are usually 1 cm (3/8") thick. The mortar mix used by the people has the following volumetric proportions:1:2:6 (cement: lime: sand). It is worth noting that the proportion used for non-engineered construction in Mexico does not satisfy the minimum volumetric requirements proposed by NTCM-2004 [12], but it is used as it is an inexpensive mortar and workability is good. However, it is also worth noting that this mortar mix has better volumetric proportioning than mortar type O (1:2:9) allowed by masonry codes of the United States like ACI 530-14 [13] for non-seismic regions.

The best mortar mix proportion (a volumetric mortar mix 1:¼:3½) recommended by NTCM-2004 [12] for structural application, known as "Mortar Type I" was also used. The purpose of using this mix is that most lateral loading cyclic tests conducted in Mexico for confined masonry walls have used this mortar type [5-11], and cross comparisons with the dominant masonry construction in Mexico is also desirable.

Therefore, it was also necessary to assess physical and mechanical properties of the materials and the masonry used in this type of construction, as well as determine these properties if a code-based mortar mix is used. These testing are documented in detail elsewhere [1-3], and is summarized in Tables 1 to 6.

Property	Bricks	Blocks
Number of Tested Units	19	18
Volumetric Weight γ (Ton/M^3)	1.57	1.08
Absorption	18.3%	26.5%
Initial Rate of Absorption (Gr/Min)	59.4	32.7
Saturation Coefficient	0.94	0.94
Modulus of Rupture, F_r (MPa)	0.86	0.96
Compressive Strength		
Mean: $\overline{f}_p$ (MPa)	10.1	4.2
Design: f^*_p (MPa)	5.4	2.4

Table 1. Index properties for bricks and blocks

Property	Type I	Non-Engineered
Number of Cubes	30	35
Volumetric Weight γ (Ton/M^3)	1.57	1.51
Compressive Strength		
Mean: $\overline{f}_j$ (MPa)	24.1	7.8
Design: f_j^* (MPa)	13.4	4.3

Table 2. Index properties for mortar

Mexican standards are similar to ASTM guidelines, particularly in testing procedures; however, they differ in the sampling and statistical criterion, particularly to define mechanical design properties denoted with and asterisk (*).

For example, the design compressive strength of a masonry unit f_p^* according to NTCM-2004 [12] should be computed as:

$$f_p^* = \frac{\overline{f}_p}{1 + 2.5c_p} \tag{1}$$

where $\overline{f}_p$ is the mean value from test results and c_p is the coefficient of variation of the test results that shall not be taken less than recommended minimum values established by NTCM-2004. As the c_p value obtained during test results [1, 2] was smaller than the minimum values allowed by NTCM-2004, then minimum values established by NTCM-2004 [12] were used for the reported values in Table 1, that is, $c_p = 0.3$ was used for concrete blocks (mechanized production with no quality control) and $c_p = 0.35$ for the fired clay bricks (non-industrial production).

2.1 Axial compression prism tests

Given the particularity of the combined masonry, where brick layers alternate with block layers, and that bricks and blocks have very different properties (Table 1), two different arrangements were constructed for each mortar type used (Figure 5). It is worth noting that guidelines worldwide for masonry prism tests assume that the same material (brick or block) is used to build the prisms, so combined masonry is not really fully addressed at this time.

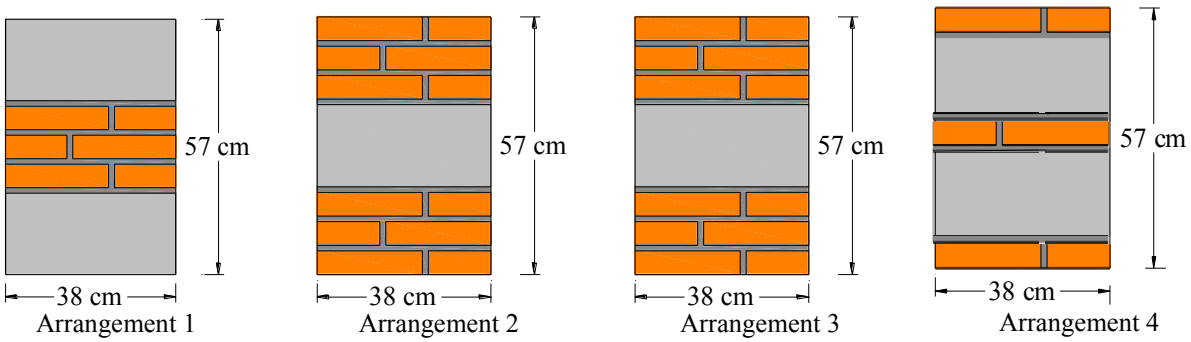

Figure 5. Prisms arrangements for the walls under study

Nine prisms were tested for each arrangement, according to the minimum required by NTCM-2004. The slenderness ratio for the prisms was 4.78, within the range $2 \le h/t \le 5$ established by NTCM-2004.

Test results for prisms with mortar type I are summarized in Table 3, where it can be observed that although higher values for the mechanical properties are obtained under arrangement 1, differences are no significant: around 20% for compressive strength and 5% for the modulus of elasticity. Therefore, for practical purposes it would be convenient to take the weighted properties obtained from the data of both arrangements, that is, f^*_m=19.7 kg/cm^2 (1.9 MPa) and E_m=12,245 kg/cm^2=1,201 MPa (E_m=621.6f^*_m).

Arrangement	$\overline{f}_m$	c_m	f^*_m	E_m
	MPa		MPa	MPa
1	3.1	0.15	2.2	1,233
2	2.6	0.17	1.8	1,171
1 and 2	2.8	0.18	1.9	1,201

Table 3. Index properties from prism tests using mortar type I

Test results for prisms with non-engineered mortar are summarized in Table 4, where it can be observed that there are no differences between arrangements 3 and 4 for practical purposes. Therefore, the weighted properties obtained from the data of both arrangements are f^*_m=15.7 kg/cm^2 (1.5 MPa) and E_m=15,572 kg/cm^2 =1,527 MPa (E_m=991.8f^*_m).

Arrangement	$\overline{f}_m$	c_m	f^*_m	E_m
	MPa		MPa	MPa
3	2.3	0.20	1.5	1,604
4	2.3	0.20	1.5	1,458
3 and 4	2.3	0.19	1.5	1,527

Table 4. Index properties from prism tests using non-engineered mortar

It is worth noting that there are no significant differences between the design compressive strength f^*_m for the prisms built with mortar type I and non-engineered mortar, as it is around 25.5%, perhaps good enough for design under gravitational loading.

2.2 Diagonal compression wallet tests

According to NTCM-2004 [12], small square masonry subassemblies (wallets) as depicted in Figure 6 can be tested under axial compression (commonly using an universal press machine) in order to define an indirect shear (diagonal tension) strength v^*_m for design and the shear modulus G_m.

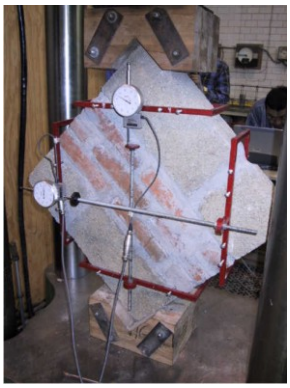

Figure 6. Axial compression test of NTCM-2004 to determine v^*_m and G_m.

Given the particularity of the combined masonry and the reasons stated in the previous section, two different arrangements of wallets were also constructed for the diagonal compression tests for each mortar type used (Figure 7).

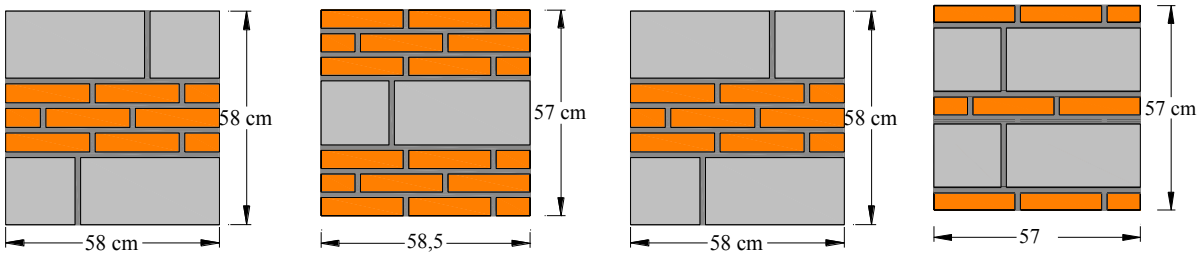

a) Mortar Type I b) Non-engineer Mortar

Figure 7. Small wallet arrangements built for axial compression tests

The arrangements were selected based upon the combined masonry walls that were finally tested (Figures 8a and 8b). Nine specimens were tested under diagonal compression for each arrangement, according to the minimum required by NTCM-2004. The aspect ratio for the specimens was almost square, as recommended by NTCM-2004.

Test results for specimens jointed with mortar type I are summarized in Table 5, where it can be observed that, in contrast to what was observed from prism tests, important differences are obtained for shear strength indices values v^*_m between the small wallet arrangements 1 and 2. The most notorious scatter of the data and the smallest values were obtained for arrangement 1. These can be explained by the different predominant modes of failure observed in the tested specimens. For arrangement 1, the predominant mode of failure was sliding along bed joints, whereas for arrangement 2 the predominant mode of failure was diagonal tension. In contrast, no important differences were observed between arrangements 1 and 2 to obtain the average shear modulus G_m (Table 5).

Arrangement	$\bar{v}_m$ **MPa**	c_v	v^*_m **MPa**	G_m **MPa**
1	0.28	0.51	0.13	420
2	0.38	0.18	0.25	393
1 and 2	0.33	0.37	0.17	415

Table 5. Index properties from diagonal compression tests using mortar type I

Test results for specimens jointed with non-engineered mortar are summarized in Table 6, where it can be observed that differences are also obtained for shear strength indices values between the small wallet arrangements 3 and 4. The most notorious scatter of the data and the smallest values were obtained for arrangement 4. However, in contrast to what was observed for mortar type I, a predominant mode of failure was not observed in the tested specimens, as failures in diagonal tension and sliding along bed joints were observed for both arrangements 3 and 4. A 35% difference is observed between the average shear modulus G_m obtained for arrangements 3 and 4 (Table 6), in contrast to what was observed for mortar type I.

Test results lead one to conclude that there is a reasonable doubt on how representative is the axial compression test to define shear strength indices for combined masonry, which can only be answered by relating these index values to estimate the lateral shear strength of wall specimens subjected to lateral loading, as shown in following sections.

Arrangement	$\bar{v}_m$ MPa	c_v	v^*_m MPa	G_m MPa
3	0.27	0.29	0.16	417
4	0.25	0.44	0.12	310
3 and 4	0.26	0.35	0.14	367

Table 6. Index properties from diagonal compression tests using non-engineered mortar

3 TEST SPECIMENS

Four walls were constructed and tested under cyclic lateral loading. The cryptogram for identification of each wall is MCC-*i* , where *i* is an index to identify the number of wall sequentially tested. The first two walls (MCC-1 and MCC-2) were jointed with mortar type I and the last two walls (MCC-3 and MCC-4) with non-engineered mortar.

The geometry of the walls is schematically depicted in Figure 8. The general dimensions of walls and their confinement elements were selected to make these walls as close as possible to the dimensions of a confined brick masonry wall previously tested [7] at Cenapred (wall M-0-E6), to do some cross comparisons.

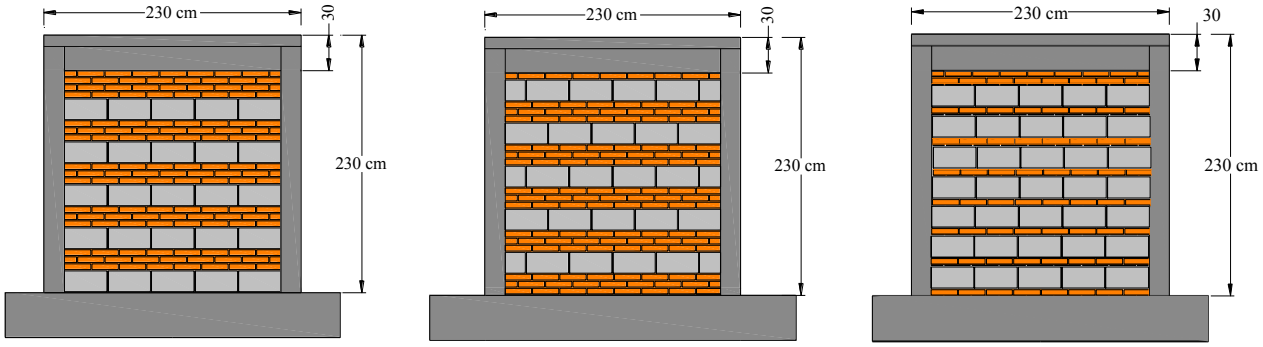

a) Walls MCC-1 and MCC-3 b) Wall MCC-2 c) Wall MCC-4

Figure 8. General geometry of tested walls

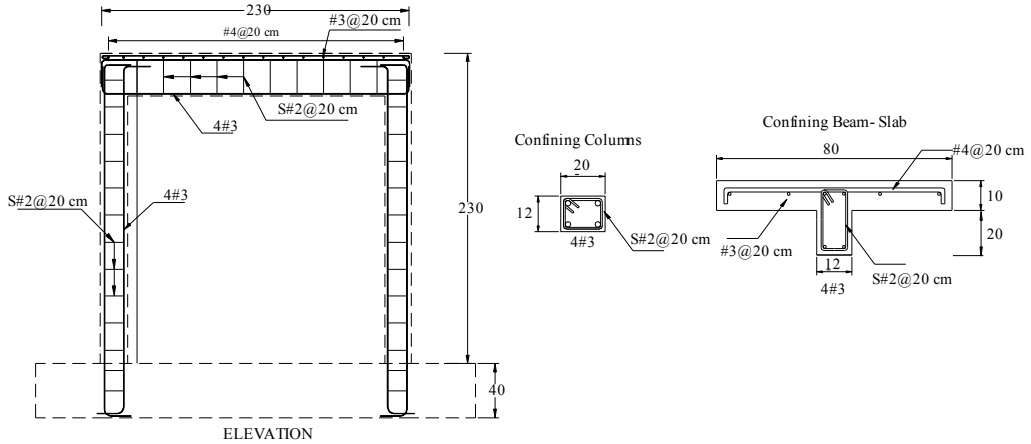

Figure 9. Reinforcement of confining elements

In fact, the confining RC tie-columns, bond-beam and beam on grade have the same dimensions, reinforcement and concrete strength with respect to those of the wall of reference [7], as depicted in Figure 9 and specified in Table 7. Confining tie-column elements are 12x20 cm. The confining rectangular bond-beam is 12x20 cm. A slab 10x80 cm was cast at the top of the confining beam. The compressive strength of the concrete used for the confining tie-

columns and bond-beams was specified as f'_c=150 kg/cm^2 (14.7 MPa) and for the slab was f'_c=250 kg/cm^2 (24.5 MPa). Results of controlled cylinder tests are reported elsewhere [1, 2].

Columns		Beam		Slab	
Longitudinal	Transverse	Longitudinal	Transverse	Longitudinal	Transverse
4#3	S#2@ 20 cm	4#3	S#2 @ 20 cm	#3 @ 20 cm	#4 @ 20 cm

Notes: #3 bars = bars 3/8" in diameter, f_y = 412 MPa
#2 bars= bars 2/8" in diameter, f_y = 216 MPa

Table 7. Reinforcement of the confining RC elements of walls

The external instrumentation for the walls was composed of 8 LVDT (Figure 10a) and a load cell (Figure 11). The internal instrumentation consisted of 12 strain gages placed on the longitudinal reinforcement of the confining elements, as depicted in Figure 10b.

The testing of the walls was done with the help of the reaction braced frame and strong floor schematically depicted in Figure 11. A special C steel beam was designed to apply a uniformly distributed vertical loading of 1 Ton/m (9.81 kN/m) and to help applying with a hydraulic jack the cyclic lateral loading.

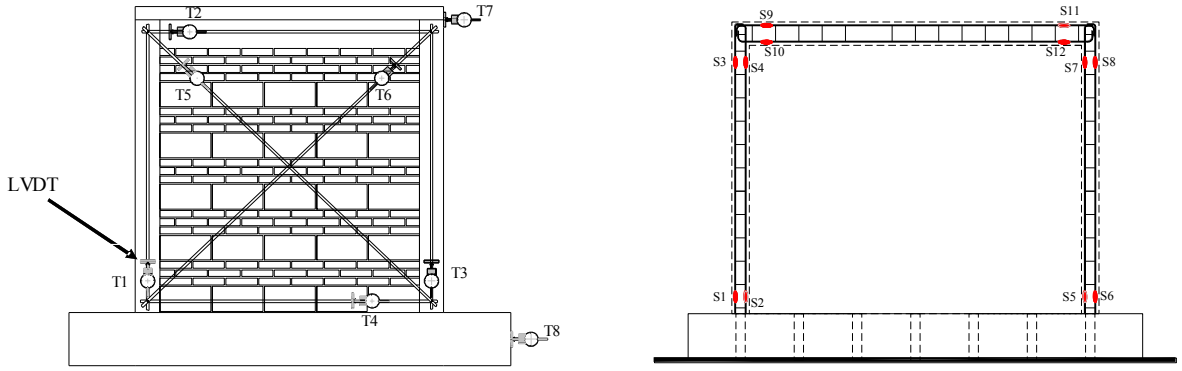

a) External wall instrumentation b) Internal wall instrumentation

Figure 10. Instrumentation for the walls

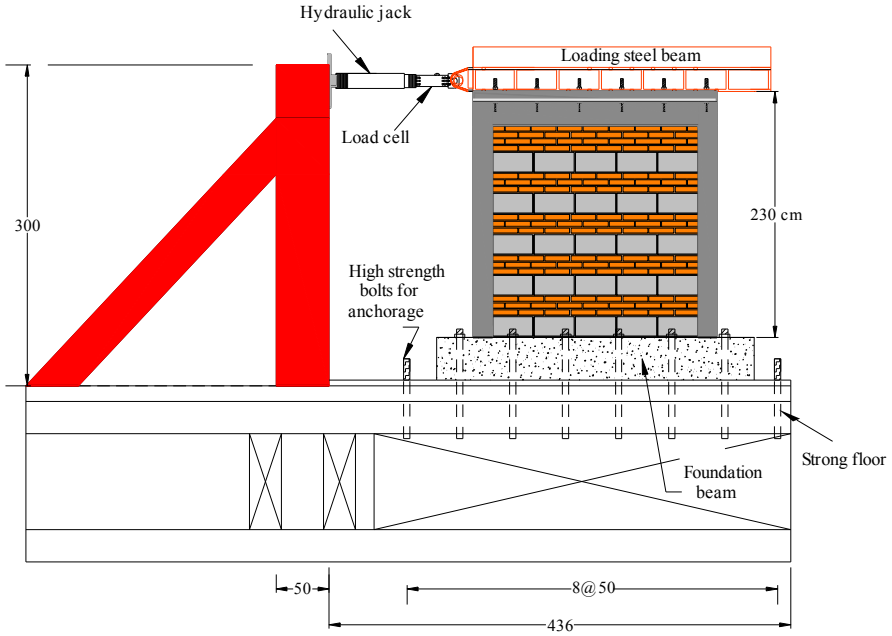

Figure 11. Testing setup

The cycling testing of the walls was done following the general guidelines of Appendix A of NTCM-2004 [12] required for earthquake-resistant masonry wall systems. According to the testing protocol of reference, masonry walls have to be subjected to repeated cycles of at least 25%, 50% and 100% the estimated cracking load for the walls (load control, Figure 12) and, after the first cracking, walls have to be subjected to repeated cycles of increasing drift ratios of at least 0.2% (displacement control, Figure 12). In this research, both the load and the displacement control were done using additional steps, as schematically illustrated in Figure 12.

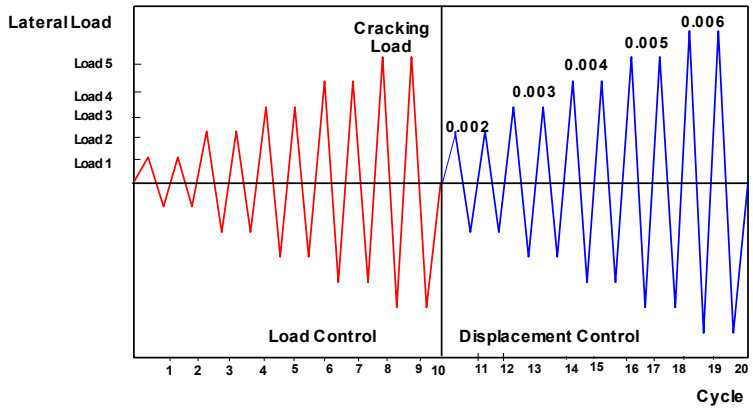

Figure 12. Cyclic testing protocol used

4 EXPERIMENTAL RESULTS

4.1 Hysteretic behavior

The hysteretic loops obtained for each wall from the cyclic testing protocol described before are depicted in Figure 13. Given the limitations of lab equipment at the time of each testing, it is worth noting the following observations regarding the testing of each wall. During the testing of wall MCC-1 a load cell was not available, so applied lateral forces were obtained indirectly from a previously calibrated manometer, that is why the curves in Figure 13a look rough. During the testing of wall MCC-2 the hydraulic jack "stock" for positive cycles (pulling) after a lateral drift angle of 0.4%, so that is the reason of the asymmetric loops, which are marked with a red-broken line. Fortunately, there were no further technical problems during the testing of walls MCC-3 and MCC-4.

From all the hysteretic loops it is observed a reasonably symmetric and stable response for positive and negative cycles up to a drift angle of 0.6%, except for wall MCC-2 for the reason stated above (loops were rather symmetric up to a drift angle of 0.4%, where the jack problem aroused).

Instability in the wall response triggered for a drift angle of 0.6% for wall MCC-1 after a major shear crack penetrated the confining column (Figure 14); this last half cycle is marked with a broken red line in Figure 13a.

The instability of wall MCC-2 also started because of a shear crack penetration in the confining column at a drift ratio around 0.6%, where an important strength and stiffness degradation was observed (Figure 13b).

For wall MCC-3 an important pinching behavior triggered after a lateral drift of 0.4% (Figure 13c) and the important shear crack penetration of the confining column started at a drift of 0.5%, the testing was stopped at a drift of 0.6% as extensive damage with crack penetration of top and bottom of the confining column was evident.

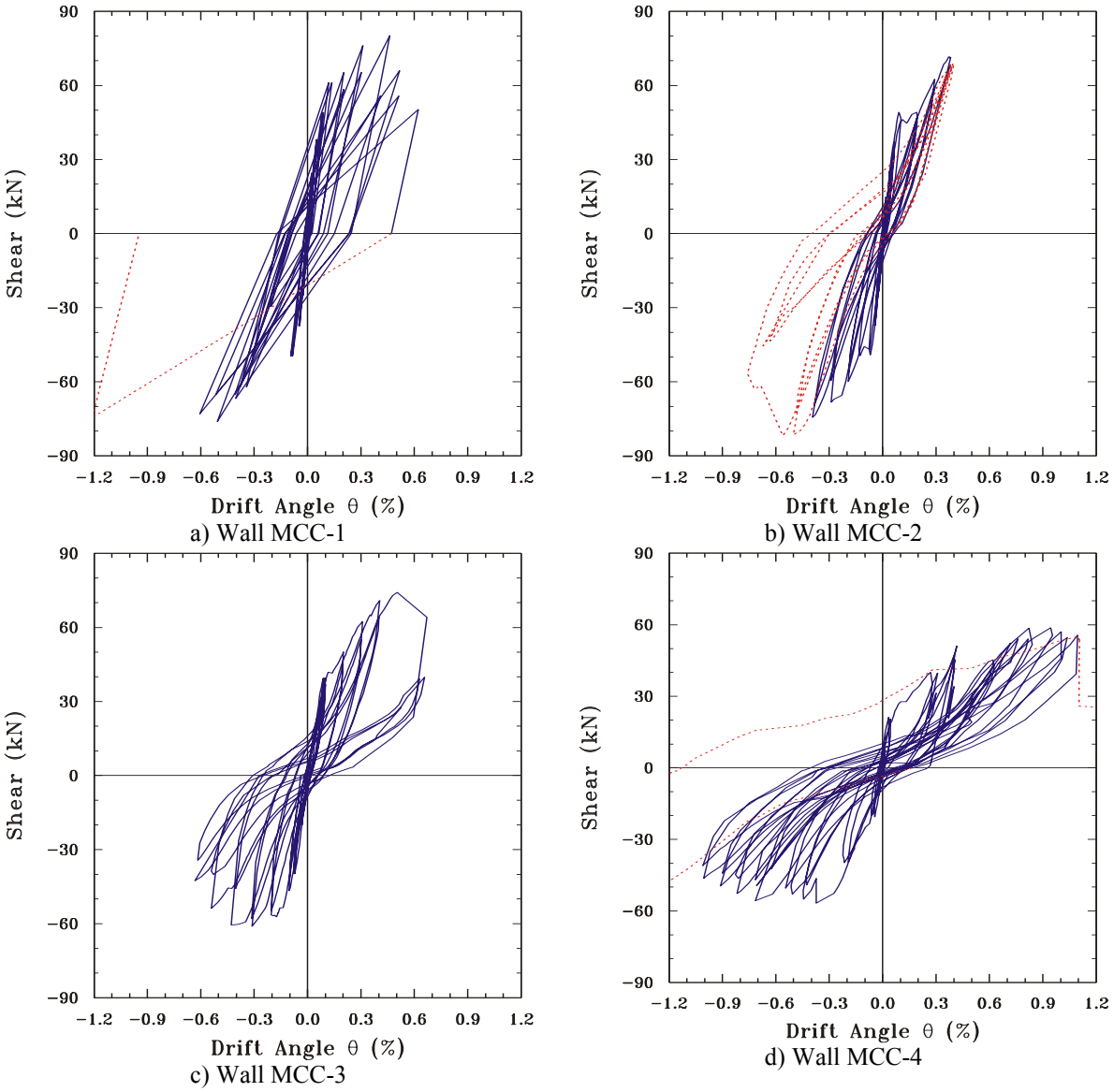

a) Wall MCC-1 b) Wall MCC-2

c) Wall MCC-3 d) Wall MCC-4

Figure 13. Hysteretic loops for the tested walls

a) Top right corner b) Bottom left corner

Figure 14. Shear crack penetration of confining RC columns of wall MCC-1 that lead to failure

For wall MCC-4, an important pinching behavior was developed after a drift angle of 0.4% (Figure 13d), basically a frictionless sliding mechanism along bed and head joints during load reversals of a stair-like shear cracking pattern (significant gaps were observed during testing,

particularly at the head joints). Although the important shear crack penetration at the confining column happened at a lateral drift of around 0.6%, this wall presented a very important frictionless sliding mechanism along the bed and head joints that allowed it to sustain stability up to a drift angle of 1%, after that the wall failed because of the shear crack penetration of the confining RC column (dotted red lines, Figure 13b).

4.2 Cracking patterns

The final cracking patterns for all tested walls are depicted in Figure 15, where it can be observed that they are typical diagonal tension shear patterns. It is also worth noting that the shear crack that penetrated the confining column elements started to appear in all walls at a drift angle as low as 0.3%.

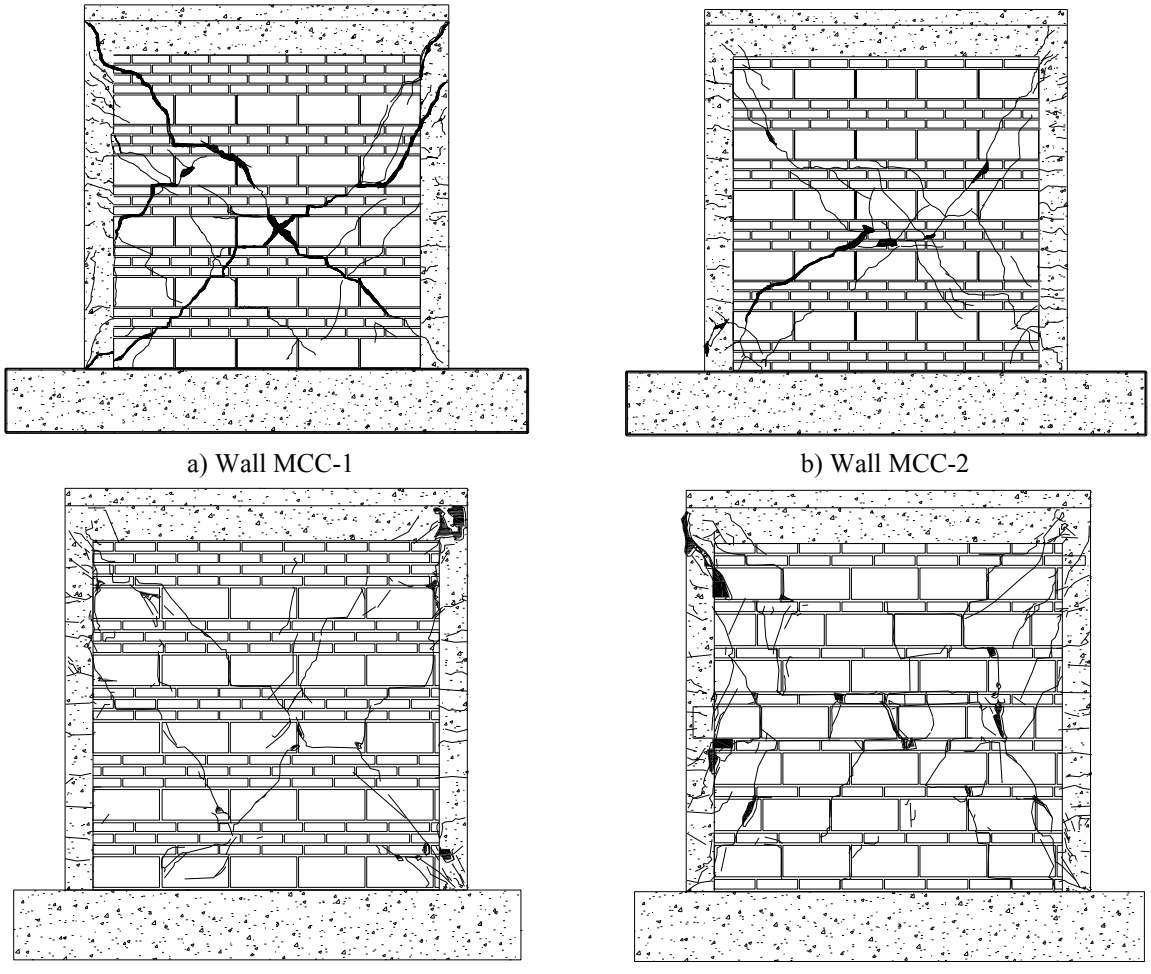

a) Wall MCC-1 b) Wall MCC-2

c) Wall MCC-3 d) Wall MCC-4

Figure 15. Final cracking patterns of tested walls

From a gross assessment viewpoint, from the crack patterns, the obtained hysteretic loops and the response envelopes (not shown), it can be observed that the main difference in the cyclic behavior of the walls jointed with mortar type I of NTCM-2004 (walls MCC-1 and MCC-2) and the walls jointed with non-engineered mortar is due to the diagonal crack pattern exhibited for the walls. A well-defined main diagonal crack that crosses and breaks bricks and block layers are developed for the walls jointed with the stronger engineered mortar (walls MCC-1 and MCC-2, Figures 15a and 15b). In contrast, a stair-like, frictionless sliding joint

cracking patterns are developed for the walls jointed with the weaker non-engineered mortar (walls MCC-3 and MCC-4, Figures 15c and 15d), particularly for wall MCC-4 (Figure 15d). This frictionless sliding joint mechanism during load reversals was favored because of the relatively low applied normal stress. That is the reason why more pinching is observed in the hysteretic loops of the walls joined with non-engineered mortar (Figure 13).

4.3 Characteristic parameters from response envelopes

Walls MCC-1 and MCC-2 first cracked at a higher drift angle and shear force than walls MCC-3 and MCC-4 (Table 8). In fact, walls MCC-1 and MCC-2 also developed slightly higher shear forces than walls MCC-3 and MCC-4 (Table 8). However, the difference between the shear force resisted by walls MCC-1 and MCC-3, that have the same configuration, is only 8%.

Wall	First Cracking		Peak Shear Force			
	V_{cr} (KN)	θ_{cr}	V^{+}_{max} (KN)	θ^{+}	V^{-}_{max} (KN)	θ^{-}
Mcc-1	49.0	0.0009	80.4	0.0046	76.5	0.0054
Mcc-2	49.0	0.0009	71.6*	0.0038*	82.4	0.0056
Mcc-3	39.2	0.0006	74.5	0.0050	60.8	0.0031
Mcc-4	21.6	0.0006	58.8	0.0090	57.9	0.0070
* Previous reported problem with the hydraulic jack during testing						

Table 8. Characteristic parameters obtained from peak response envelopes

The major difference regarding peak shear forces is observed between walls MCC-3 and MCC-4, which were both jointed with non-engineered mortar, where the difference is 26% (Table 8). This higher difference seems directly related to the fact that a different masonry combination exist where more blocks (weakest material) are used in wall MCC-4 with respect to wall MCC-3.

4.4 Cyclic stiffness degradation

An important parameter for the design and evaluation of structures, masonry included, is to assess their stiffness degradation with respect to increasing drift angle. This parameter is useful to help define drift angle limits for design purposes (i.e., serviceability, collapse prevention, etc). Therefore, from the hysteretic curves depicted in Figure 13, peak-to-peak secant stiffnesses were defined for each cycle at the same drift angle, and then normalized with respect to the computed initial (elastic) stiffness for each walls. The computed curves for all walls are depicted in Figure 26, where first and second cycles at the same drift angle are plotted in separate curves.

It can be observed from Figure 16 that there are no significant differences between the curves of the first and second cycles for all walls except wall MCC-4. The lateral stiffness of all walls degrades very fast, being 0.4 or less of its initial uncracked stiffness K_e for a drift angle as low as 0.2%. For the drift angle where the shear crack starts to penetrate the confining column elements (θ=0.3%), the K/K_e ratio is lower than 0.3 for the walls joined with engineered mortar (walls MCC-1 and MCC-2, Figures 16a and 16b), whereas the walls joined with non-engineered mortar developed a K/K_e ratio higher than 0.3 (walls MCC-3 and MCC-4, Figures 16c and 16d). Spalling of masonry started close to a drift angle of 0.4% or less, where all walls have $K/K_e < 0.25$.

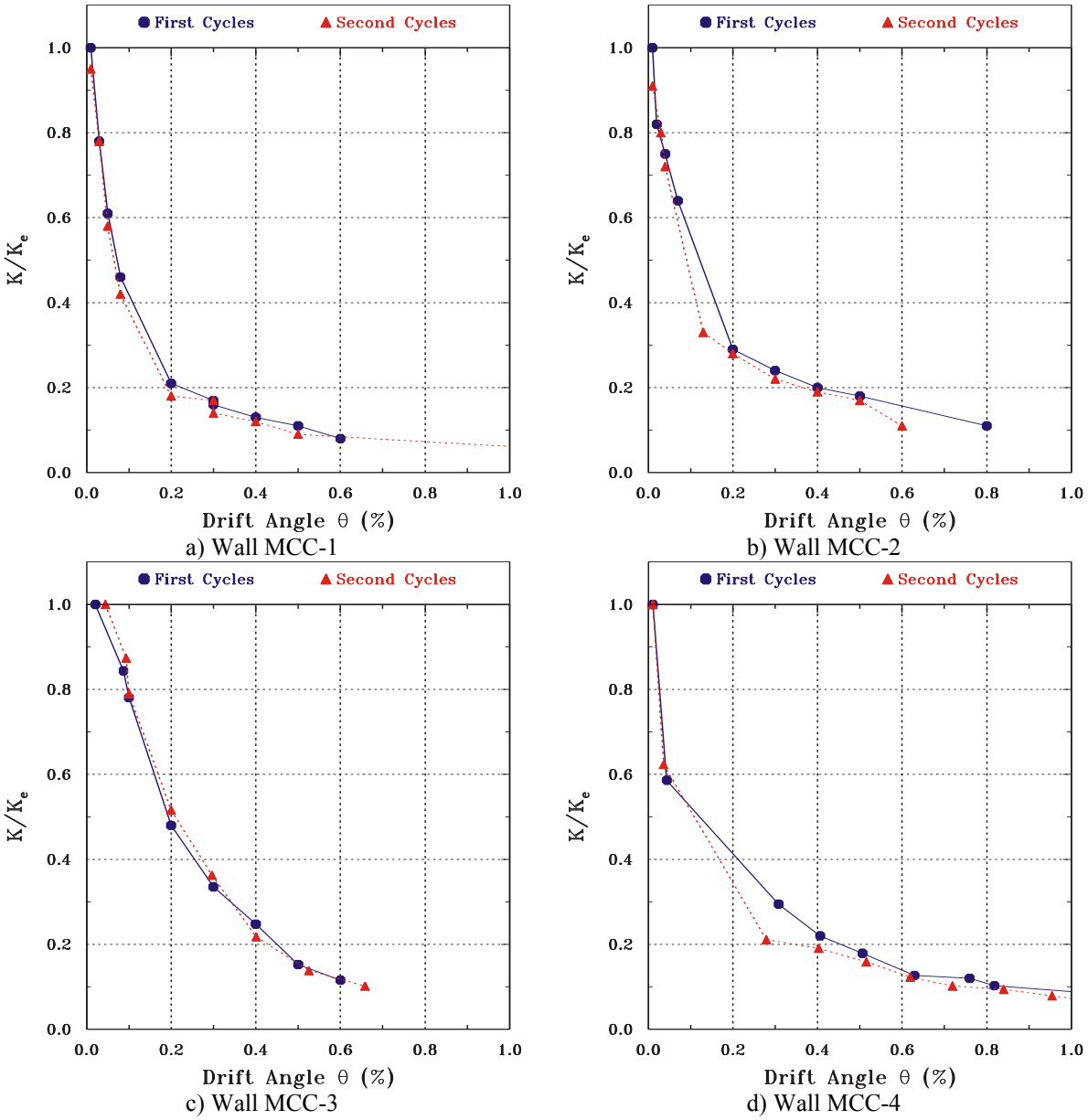

Figure 16. Normalized peak-to-peak secant stiffness vs. drift angle for tested walls

5 DAMAGE INDEX

Structural engineers need simple quantitative evaluation methods to assess the safety of existing structures under an expected level of seismic demand, particularly to take decisions regarding rehabilitation and/or demolition. Damage indices are suitable tools for such purposes.

Therefore, the damage index originally proposed by Kwok and Ang [14] for unreinforced brick masonry walls based on a reliable database of experiments conducted in China in the late 1970s was calibrated with the experimental data obtained in this research study for confined and combined masonry walls.

The Kwok-Ang damage index is defined with the following general expressions:

$$D = D_u + D_e \tag{2}$$

$$D_u = \frac{u_m}{u_f} \tag{3}$$

$$D_e = \varepsilon \frac{\int dE}{q_u u_f} \tag{4}$$

where u_m is the displacement at maximum load, u_f is the displacement at failure, $\int dE$ is the total (cumulative) dissipated energy, q_u is the ultimate shear strength and ε is a constant obtained from regression analysis of experimental data.

Kwok and Ang [14] obtained from the regression analysis of their extensive database that ε=0.075 for unreinforced masonry walls. In addition, they proposed the following damage scale for their index: a) No damage: $D = 0$, b) Reparable damage: $0 < D \leq 0.25$, c) Severe damage: $0.25 < D < 1.0$, d) Collapse: $D \geq 1$.

It is clear that there are some differences in the cyclic behavior under lateral loading of plain unreinforced masonry and the combined and confined masonry described in this study, so some adjustments to the damage index originally proposed by Kwok and Ang were needed for combined and confined masonry walls. For example, the value of constant ε should be assessed from experimental data. Also, the limiting boundary value between reparable and severe damage should be also redefined with the observed experimental behavior to take into account the beneficial presence of confining elements that provide further stability in these walls under lateral loading.

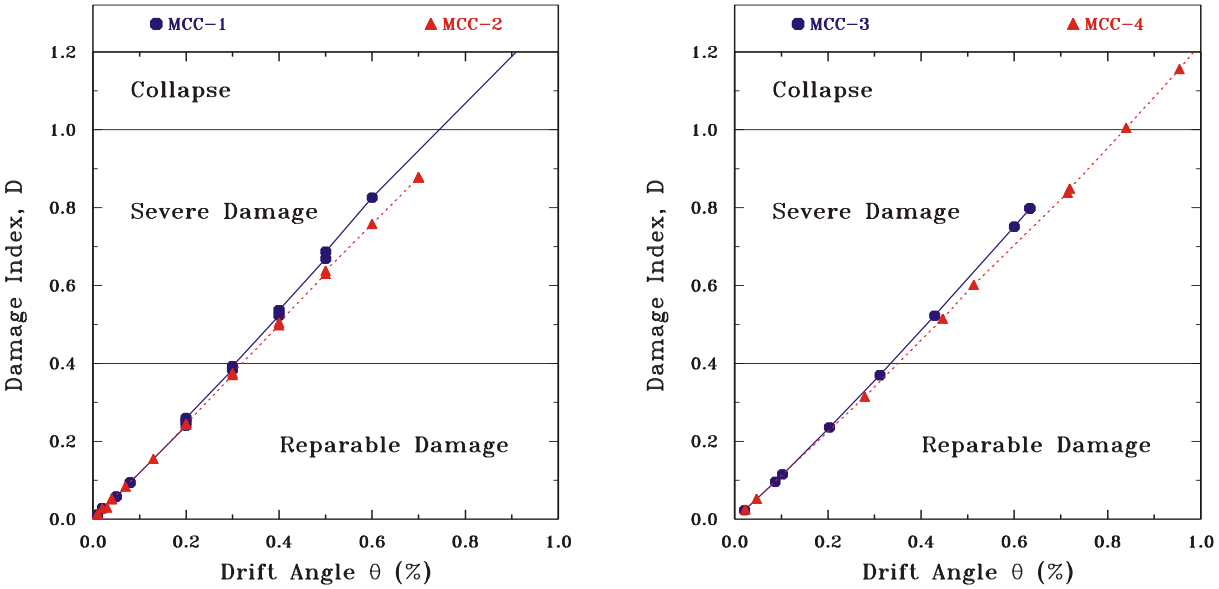

a) Walls with engineered mortar b) Walls with non-engineered mortar

Figure 17.Modified Kwok-Ang damage index vs drift angle for combined and confined masonry walls.

Therefore, from the reduced database of the experiments described here, a preliminary value of ε =0.046 was obtained for combined and confined masonry walls, as reported elsewhere [1-2]. Also, from the analysis of experimental data that allowed defining the limiting lateral drift ratio $\theta = 0.003$ for earthquake-resistant design purposes [1-3], it was clear that the limiting boundary value between reparable and severe damage should be $D = 0.4$ for combined and confined masonry. Therefore, the proposed damage index scale for combined and confined masonry is: a) No damage: $D = 0$, b) Reparable damage: $0 < D \leq 0.4$, c) Severe damage: $0.4 < D < 1.0$, d) Collapse: $D \geq 1$. The obtained damage index vs. drift ratio curves for the tested combined and confined masonry walls are depicted in Figure 17, where it can be

observed the proposed adjustments for the Kwok-Ang damage index seem reasonable for both the walls jointed with engineered (Figure 17a) and non-engineered (Figure 17b) mortar.

6 CONCLUDING REMARKS

From the experimental program summarized in this paper, the following observations can be made:

1. The major difference in the cyclic behavior of the combined and confined masonry walls jointed with engineered and non-engineered mortar is related to the resisting shear mechanism that leads to failure. In the walls jointed with engineered mortar, the failure mechanism is characterized by diagonal tension cracks that favor primarily spalling and crushing of the masonry in the central zone of the main diagonal crack with reasonable energy dissipation characteristics. In contrast, in the walls jointed with non-engineered mortar, the initial diagonal tension cracks that broke the masonry units lessened after a drift ratio θ=0.003, when a stair-like shear mechanisms with friction-less sliding along the bed and head joints triggered, leading to an important pinching of the hysteretic loops and therefore, a reduced energy dissipation characteristics due to the low normal compression stress applied to the walls.
2. From the different wall combinations tested for combined and confined masonry walls jointed with non-engineered mortar (walls MCC-3 and MCC-4), it was observed that wall MCC-3, that has more brick layers, resisted a peak shear force 26% higher than wall MCC-4, that has more concrete blocks. Therefore, this difference seems to be directly related to the fact that a different masonry combination exists where more blocks (weakest material) are used in wall MCC-4 with respect to wall MCC-3.
3. Given that the mechanical properties of the concrete blocks currently used in combined and confined masonry walls are very weak, it will be worth testing in the future combined and confined masonry walls where higher quality concrete blocks are used, to discern if this practice would lead to improved performances under lateral cyclic loading.
4. It was shown that the Kwok-Ang damage index for unreinforced brick masonry walls can be adjusted in a simple manner, as proposed in this paper, to be helpful for the seismic evaluation of combined and confined masonry walls also.

Extensive additional experimental research is needed to discern the impact of many variables, but this research study lead one to believe that the following variables are important to assess in future experimental works: (a) the impact of other wall combinations, (b) the impact of the applied axial load, (c) the impact of other mortar mixes allowed by seismic codes and, (d) the impact of using concrete blocks of better quality, with similar mechanical properties to the ones of clay bricks. Reference confined masonry walls made of: (a) bricks only and, (b) concrete blocks only should be included in the future testing protocols.

7 ACKNOWLEDGEMENTS

This experimental study was possible because of the enthusiastic collaboration of several students and technicians at Universidad Autónoma Metropolitana. Technicians Leopoldo Quiroz (RIP), Rubén Barreda and José Luis Caballero assisted us in all the prototype and material testing. Prof. Hans Archundia-Aranda assisted us in the planning and in data acquisition of the cyclic tests. The construction of test specimens was possible because of the enthusiastic collaboration of several students: César Carpio, José Manuel Alonso, Misael Bahena, Daniel Miranda, Sergio López, Eder Gudiño, Rosaura Ramírez, Efraín Joaquín Diego, Marco Antonio Rico, René Espinoza, Richard Véliz, Roberto Moreno, Elías Josué Moral and Gerardo Ibarra.

REFERENCES

[1] A. Juárez-Ángeles, Mecanismos de resistencia y de deformación de muros de mampostería combinada y confinada, *MSc. Thesis*, División de Ciencias Básicas e Ingeniería, Universidad Autónoma Metropolitana Azcapotzalco, 2009. (in Spanish)

[2] V. H. Salinas-Vallejo, Comportamiento ante cargas laterales de muros de mampostería combinada unidos con morteros de autoconstrucción, *MSc. Thesis*, División de Ciencias Básicas e Ingeniería, Universidad Autónoma Metropolitana Azcapotzalco, 2009. (in Spanish)

[3] A. Tena-Colunga, A. Juárez-Ángeles, V. H. Salinas-Vallejo, Cyclic behavior of combined and confined masonry walls, *Engineering Structures*, **31** (1), 240-259, doi:10.1016/j.engstruct.2008.08.015, 2009.

[4] A. Tena-Colunga, A. Juárez-Ángeles, V. H. Salinas-Vallejo, Housing Report: Combined and confined masonry structures, *World Housing Encyclopedia, an Encyclopedia of Housing Construction in Seismically Active Areas of the World*, Earthquake Engineering Research Institute (EERI) and International Association for Earthquake Engineering (IAEE), Report No. 160, 1-15, 2010.

[5] S. M. Alcocer, R. Meli, Test program on the seismic behavior of confined masonry structures, *The Masonry Society Journal*, **13** (2), 68-76, 1995.

[6] S. M.. Alcocer, Implications derived from recent research in Mexico on confined masonry structures, *Proceedings, CCMS Symposium*, American Society of Civil Engineers, Chicago, 82-92, 1996.

[7] G. Aguilar, R. Meli, R. Diaz, R. S. Vazquez-del-Mercado, Influence of the horizontal reinforcement on the behavior of confined masonry walls, *Proceedings, 11th World Conference on Earthquake Engineering*, Acapulco, Mexico, Paper No. 1380, CDROM, 1996.

[8] L. E. Flores, S. M. Alcocer, Calculated response of confined masonry structures, *Proceedings, 11th World Conference on Earthquake Engineering*, Acapulco, Mexico, Paper No. 1830, CDROM, 1996.

[9] S. M. Alcocer, J. A. Zepeda, Behavior of multi-perforated clay brick walls under earthquake-type loading, *Proceedings, Eighth North American Masonry Conference*, Austin, Texas, EUA, CDROM, 1999.

[10] S. M. Alcocer, J. G. Arias, A. Vazquez, Response assessment of Mexican confined masonry structures through shaking table tests, *Proceedings, 13th World Conference on Earthquake Engineering*, Vancouver, Canada, Paper No. 2130, CDROM, 2004.

[11] E. L. Treviño, S. M. Alcocer, R. Larrúa, L. E. Flores, Estudio experimental de muros de mampostería confinada de bloques de concreto. Primera parte: comportamiento general de los especímenes, *Ingeniería Civil*, Centro de Estudios y Experimentación de Obras Públicas CEDEX, Ministerio de Fomento, Madrid, España, No. 150, ISSN 0213-8468, 2008. (in Spanish)

[12] NTCM-2004, Normas Técnicas Complementarias para Diseño y Construcción de Estructuras de Mampostería*, Gaceta Oficial del Distrito Federal*, October, 2004. (in Spanish)

[13] ACI 530-14, Building Code Requirements for Masonry Structures (ACI 530-14/ASCE 5-14/TMS 402-14), *American Concrete Institute*, 2014.

[14] Y.-H.- Kwok, A. H.-S. Ang, Seismic damage analysis and design of unreinforced masonry buildings, *Structural Research Series No. 536*, University of Illinois at Urbana-Champaign, June, 1987.